J Paleolimnol (2007) 37:475–490
DOI 10.1007/s10933-006-9033-6

ORIGINAL PAPER

Solar and anthropogenic imprints on Lake Masoko (southern Tanzania) during the last 500 years

Yannick Garcin · David Williamson · Laurent Bergonzini · Olivier Radakovitch · Annie Vincens · Guillaume Buchet · Joël Guiot · Simon Brewer · Pierre-Etienne Mathé · Amos Majule

Received: 7 February 2006 / Accepted: 2 June 2006 / Published online: 21 October 2006

Abstract The Masoko crater-lake in southern Tanzania provides a continuous record of environmental changes covering the last 500 years. Multi-proxy studies were performed on a 52 cm sediment core retrieved from the deepest part of the lake. Magnetic, organic carbon, geochemical proxies and pollen assemblages indicate a dry climate during the 'Little Ice Age' (AD 1550–1850), confirming that the LIA in eastern Africa resulted in marked and synchronous hydrological changes. However, the direction of response varies between different African lakes (low versus high lake-levels), indicating strong regional contrasts that prevent the clear identification of climate trends over eastern Africa at this time. Inferred changes in Masoko lake-levels closely resemble the record of solar activity cycles, indicating a possible control of solar activity on the climate in this area. This observation supports previous results from East African lakes, and extends this relationship southward. Finally, anthropogenic impact is observed in the Masoko sediments during the last 60 years, suggesting that human disturbance significantly affected this remote basin during colonial and post-colonial times.

Keywords Africa · Tropics · Lake · Paleoclimate · Little Ice Age · Solar activity · Anthropogenic disturbances

Y. Garcin (✉) · D. Williamson · O. Radakovitch · A. Vincens · G. Buchet · J. Guiot · S. Brewer · P.-E. Mathé
CEREGE, UMR 6635, CNRS-Université Paul Cézanne, BP 80, Aix-en-Provence Cedex 04 F-13545, France
e-mail: garcin@cerege.fr

L. Bergonzini
UMR 8148 IDES, CNRS-Université Paris-Sud, bât. 504, Orsay Cedex F-91405, France

A. Majule
Institute of Resource Assessment, University of Dar-es-Salaam, P.O. Box 35 097, Dar-es-Salaam, Tanzania

Introduction

There is a growing body of evidence that the Little Ice Age (LIA ca. AD 1550–1850) was recorded in Africa (Huffman 1996; Verschuren 2004). However, the precise timing of hydrological change during this ''cold'' period remains unclear, especially in East Africa, where the direction of the observed patterns of climate change varies between different regions.

Climatic changes reconstructed at Lakes Naivasha and Victoria during the last millennium have been associated to changes in solar activity (Verschuren et al. 2000; Stager et al. 2005). However, recent records covering the last millennium from Lakes Malawi and Edward indicate

that climate variability in those two regions of Africa was not directly controlled by solar forcing (Johnson et al. 2004; Russell and Johnson 2005). New and complementary climate-proxy records from Africa are therefore needed to better understand the complexity of the atmospheric circulation over this region during the LIA, and to explore a potential coupling between solar forcing and regional climate patterns.

Here, we present new late Holocene paleoenvironmental data from Lake Masoko (9°S), a strongly climate-sensitive maar from southern Tanzania (Merdaci 1998; Williamson et al. 1999; Barker et al. 2000, 2003; Bergonzini et al. 2001; Gibert et al. 2002; Thevenon et al. 2003; Vincens et al. 2003). Previous studies of the Masoko catchment and lake sediment have shown the peculiarity of this basin, where both the relatively small catchment area compared to the lake surface area, and the strong hydraulic conductivity of the catchment tuff material considerably restrict runoff erosion processes on the crater slopes (Garcin et al. 2006). As a consequence, the inputs of clastic material to the deep lake are primarily constrained by the lake-level fluctuations and their effects on the lakeshore area.

The aim of this study is to reconstruct the Masoko lake-level and climate variability for the last 500 years and to test the hypothesis of solar forcing on environmental conditions in the Rungwe region.

Study area

Lake Masoko (9°20.0′ S, 33°45.3′ E, 840 m above sea level) occupies a maar crater from the Rungwe volcanic highlands in the western branch of the Rift Valley, located 35 km north of Lake Malawi. This circular late Quaternary crater has steep slopes and a flat bottom (Fig. 1b). Most of the catchment area (70%) is presently covered by dense *Brachystegia/Uapaca* semi-deciduous woodlands (Vincens et al. 2003), typical of the Zambezian phytogeographical region (White 1983) that is characterized by a severe dry season of almost 5 months. Crops occupy the remaining 30% near the summit of the rim and the southern depression of the crater. The oligotrophic lake is closed (no surface outlet), small (diameter 700 m), deep (maximum depth 38 m) and stratified, with a thermocline located at ca. 11–16 m water depth (Delalande et al. 2005). Sensitive to rainfall changes, the modern level fluctuates seasonally between 1 and 2 m. The regional climate is strongly seasonal and controlled by the strength of the African Monsoon and the migration of the Intertropical Convergence Zone (ITCZ)

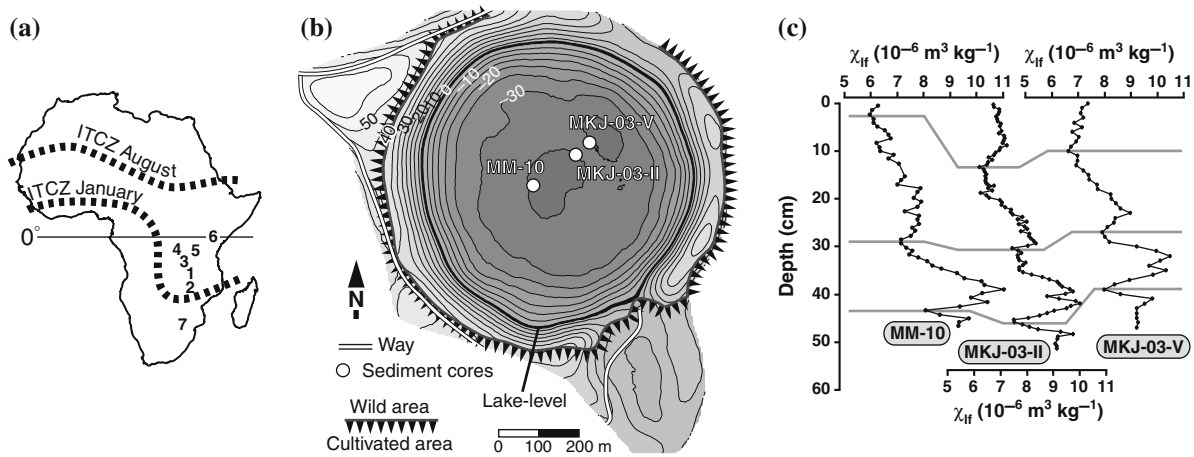

Fig. 1 (**a**) ITCZ seasonal migration over Africa. Location of Lake Masoko (1) and eastern and south-eastern African sites cited in the text: Lake Malawi (2), Lake Tanganyika (3), Lake Edward (4), Lake Victoria (5), Lake Naivasha (6) and Makapansgat Cave (7). (**b**) Lake Masoko catchment, bathymetry and cores position. (**c**) χ_{lf} profiles and correlations between three cores: Mackereth MM-10 topcore, Kajak MKJ-03-II and MKJ-03-V cores

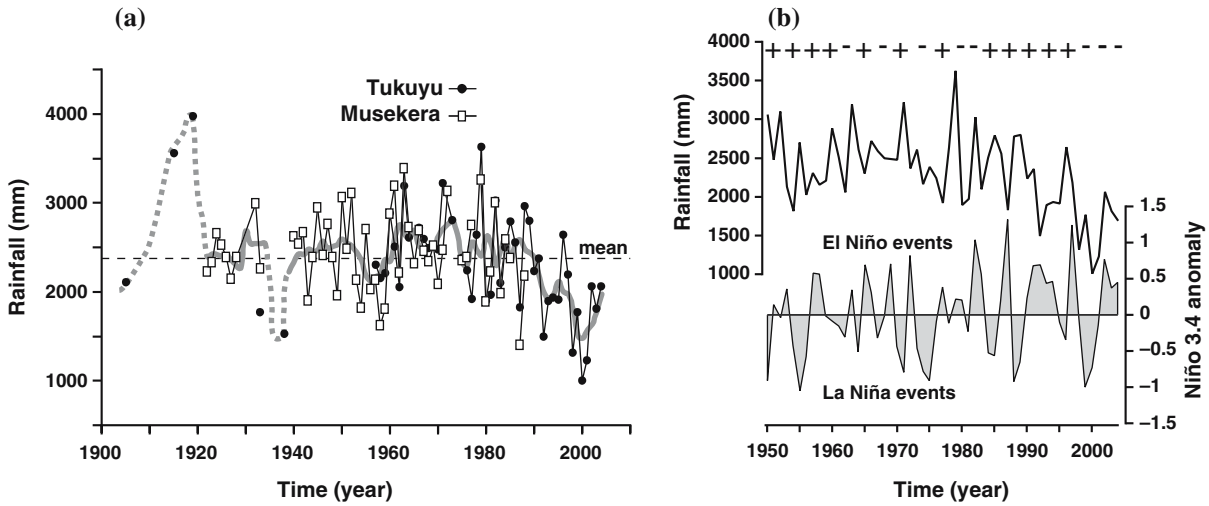

Fig. 2 (**a**) Rainfall records from the Lake Masoko area (yearly). Data compilation from Tukuyu (15 km from Masoko) and Musekera (9 km from Masoko), augmented with isolated old measurements from Tukuyu (Letcher 1918; Schnee 1920; Kanthack 1941). Thick grey lines show the 5-year averages. (**b**) Comparison between the composite rainfall from Tukuyu and Musekera at the top (yearly amounts) and the Niño-3.4 anomaly (ENSO index) at the bottom (yearly averages) (Smith and Reynolds 2004). The plus signs above rainfall data indicate wet conditions during La Niña events or dry conditions during El Niño events, while the minus signs indicate dry conditions during La Niña events or wet conditions during El Niño events

(Nicholson 1996) (Fig. 1a). The rainfall (ca. 2,400 mm year^{-1}, Fig. 2) occurs during November to May, which coincides with the insolation maximum in the southern tropics. The dry season occurs during June–October when strong trade winds provide up to 100 successive days without rainfall. Specific orographic features in the Masoko area increase the mean regional rainfall by up to 1,000 mm year^{-1}: evaporation from the large Lake Malawi to the south overloads the ascending air masses with humidity, while northern and eastern highlands favour cloud condensation and rainfall (Kerr-Cross 1891; Bergonzini et al. 2001).

The northern Lake Malawi region is highly populated: in 1925, the population density was ca. 40–60 inhabitants km^{-2} around Masoko (Gillman 1927), in 1934 it was ca. 150 inhabitants km^{-2} (Gillman 1936), and today it is estimated to be more than 300 inhabitants km^{-2} (Luifua village council, personal communication). However, since the German occupation of the Masoko area in ca. AD 1900, the inner crater basin and the lake have been protected against increasing land use activities. The present-day local population in the Masoko crater is approximately 70 people living near the crater crest (seven households), giving a population density close to the 1934 regional level. Anthropogenic activities in the Masoko crater mainly consist of cattle keeping around the lakeshores and lake-water use for household purposes such as fishing, drinking, bathing, and washing. The Luifua village council protected the inner crater from fires and tree clearance in 1996.

Materials and methods

Several ca. 50 cm long undisturbed cores, including the sediment-water interface, were collected in 1996 and 2003 in the deepest central part of the lake with a Kajak corer (Kajak 1971) and immediately sub-sampled at 5 mm depth-interval using a multi-tube rotative sampler (EMTER). This study is based on the lacustrine sediments of the 52 cm-long core MKJ-03-II (Fig. 1b, c), which are compared with catchment material (soil and tuff).

Most of the measurements were made on the original core, except the $\delta^{13}C$ analysis and the radiocarbon dates which were obtained from a duplicate core MKJ-03-IIb), correlated to the original MKJ-03-II by using measured values of total organic carbon (TOC) content.

Magnetic measurements were carried out on wet samples taken from the core and lake-bottom modern sediments, and on catchment materials (tuff, soil and eroded soil). The low-field magnetic susceptibility (χ_{lf}) was measured on a Kappabridge (KLY-2) and normalized to the dry-mass of the sample. To improve the observation of changes in terrigenous sources, the χ_{lf} was normalized to the total organic matter (TOM-free mass) of the samples, yielding $\chi_{lf(TOM\text{-}free)}$ values. Additional detailed magnetic and sedimentological measurements performed both on the catchment and sediment materials that support our interpretations are described by Williamson et al. (1999) and Garcin et al. (2006). Pollen analysis methods are described by Vincens et al. (2003).

Dried samples were pounded in a mortar and homogenized for geochemical analysis. Total nitrogen (N tot) and TOC contents were measured using a CNS elemental analyser (EuroEA, Eurovector), after removal of the carbonate fraction with a 3 and 20% HCl solution at 80°C. Biogeochemical signals in lake sediments are used to detect both natural and anthropogenic changes in the catchment and in the lake (e.g. productivity). The carbon/nitrogen (C/N) ratio of organic matter is used to differentiate terrestrial from aquatic material. Terrestrial plant material has high C/N ratios (>20) due to the presence of woody tissues, whereas C/N ratios below 15 are mainly linked to aquatic algae (Meyers 1994). TOM was estimated using loss on ignition (LOI, see below). The $\delta^{13}C$ was measured on TOC after decarbonation, using an OPTIMA spectrometer.

To determine the bulk chemistry of the lake sediments (66 samples) and catchment materials (33 samples), samples (ca. 250 mg) were weighed at 110 and 1,000°C to estimate the moisture content and LOI, respectively. Alkaline fusion was accomplished by mixing the sample with lithium metaborate (99.99% $LiBO_2$) and heating at 1,000°C during 50 min. The resulting residue was then digested using 50 ml concentrated HCl (1 N), and analysed by inductively coupled plasma optical emission spectroscopy (ICP-OES, Jobin Yvon ULTIMA C). The detection limits for all elements (<2 ppm) were well below the lowest measured concentrations in samples.

The ^{210}Pb chronology was determined for 25 samples by measuring ^{210}Pb activity through its granddaughter product ^{210}Po. Two hundred and fifty milligrams sediment were digested with acids and ^{209}Po added as a yield tracer. Polonium isotopes were deposited on a silver disc and measured by alpha spectrometry. Supported ^{210}Pb was estimated following the method of Binford et al. (1993) and was subtracted from the total ^{210}Pb to obtain unsupported ^{210}Pb. The sedimentation rate was calculated by the C.I.C. method (Krishnaswamy et al. 1971) from the portion of the core showing an exponential decrease with depth. Due to unreliable estimates of the wet sediment volume of our samples and to the loss of several samples during the core transport, we did not use the C.R.S. method which allows downcore changes in accumulation rate to be calculated. Finally, one accelerator mass spectrometry (AMS) ^{14}C date was obtained on the TOM from a single sample at 43 cm.

To further help in the interpretation of the Masoko proxies, a principal component analysis (PCA) was applied to the sedimentary parameters of core MKJ-03-II.

Results

Chronology

The total ^{210}Pb activity shows an exponential decrease with depth indicating a near constant sedimentation rate of 2.2 mm $year^{-1}$ for the first 21 cm (Fig. 3a). However, the ^{210}Pb profile suggests that the upper 4 cm are mixed, probably as a result of disturbance of the surface sediments during the Kajak (gravity) coring process. A peak in Na_2O and K_2O at 40.2 cm highlights a diffuse tephra layer (Fig. 3b), corresponding to a sanidine-rich deposit, probably originating from an eruption of the nearby Rungwe volcanoes. This tephra was correlated to the most recent ash layer of the northern Lake Malawi sediments (cores located ca. 50 km to the south), dated at AD 1674 ± 13 (see Table 1) from an annually laminated sequence (Barry et al. 2002).

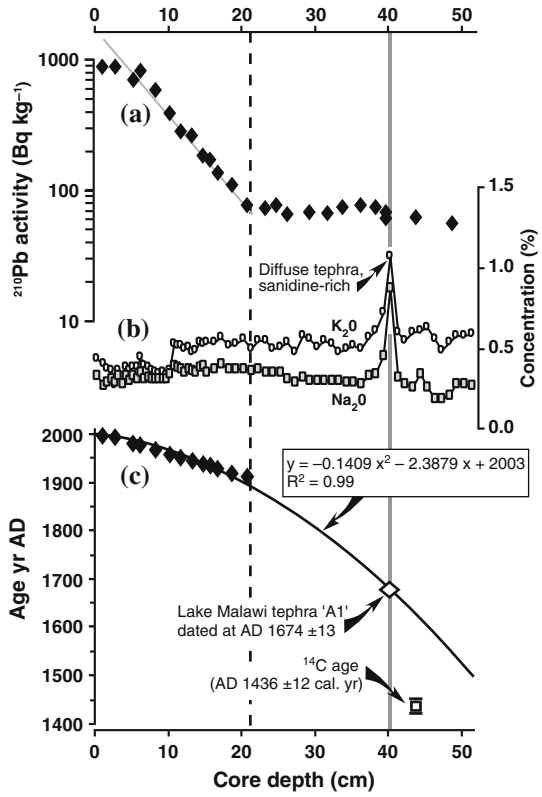

Fig. 3 Chronological framework for the core MKJ-03-II. (**a**) Total ^{210}Pb activities *versus* depth. Supported ^{210}Pb is reached at 21 cm. The average ^{210}Pb activity error is ca. 5 Bq kg^{-1}, and the error bars are hidden by the plot symbols. (**b**) A diffuse tephra layer was identified with K_2O and Na_2O concentration peaks indicating high concentration of sanidine minerals, supported by optical microscope observations. This tephra was correlated to the most recent varve-dated tephra from Lake Malawi, located 35 km to the south: i.e. tephra A1, AD 1,674 ± 13 (Barry et al. 2002). (**c**) Age-depth relation based on a polynomial curve fitted through age control points. Chronology was built using ^{210}Pb ages and the tephra layer. An outlier radiocarbon age (number H3012; 43 cm; AMS age = AD 1485 ± 35; Calibrated age: AD 1423–1448) could indicate contamination with older carbon

A radiocarbon date was obtained at 43 cm (AD 1436 ± 12 calendar years) for the base of the record. The radiocarbon date appeared to be older than expected, given the series of ^{210}Pb measurements and the tephra age, and may possibly be contaminated with old carbon from the catchment and groundwater inflow. To test this, a chronology was established using a second order polynomial passing through the ^{210}Pb and the AD 1674 tephra age only (Fig. 3c). This chronology is concordant with a progressive decrease of the apparent sedimentation rate due to the non-linear increase of compaction with depth. Further, the chronology excluding the radiocarbon date fits well with the chronology established for the long sequence from Masoko covering the last 45,000 years (Garcin et al. 2006). An alternative age model including the radiocarbon date fits poorly to the long core chronology. The first chronology has therefore been used in this study. However, due to the chronological limits of our age-depth model, the exact timing of environmental and climatic changes as discussed below should be taken with caution.

The core MKJ-03-II record

Based on changes in χ_{lf}, organic carbon content, pollen assemblages and Ti-normalized geochemical proxies (Fig. 4), two main units of respectively (i) high χ_{lf}/low native tree pollen frequencies at the bottom (unit M-2) and (ii) low χ_{lf}/high native tree pollen frequencies at the top (unit M-1) have been defined for core MKJ-03-II. Each of them has been further subdivided in subunits (M-1$_{a,b}$ and M-2$_{a,b}$). These units are superimposed on a general upward decrease of the C/N ratio and δ^{13}C profiles, which suggests a general (upward) preservation of relatively young, nitrogen-rich algal organic matter in the Masoko sequence, previously observed for a longer core by Merdaci (1998).

In the bottom M-2 unit, (52–24 cm; ca. AD 1500–1860), the sediment shows relatively high percentages of herbaceous pollen (mainly grasses) and relatively high χ_{lf} values. In addition, values in the χ_{lf}, organic carbon and geochemical records are highly variable, and display characteristic and synchronous oscillations.

Sub-unit M-2$_b$ (52–43 cm; ca. AD 1500–1650) is characterized by maximum χ_{lf} values, although it also includes a χ_{lf} minimum at 45 cm. The same oscillation is observed in the Si/Ti, Al/Ti, Nb/Ti and Fe/Ti profiles, while values of LOI, N tot and TOC show opposing fluctuations. In this interval, the native tree pollen frequencies are the lowest in the record.

In M-2$_a$ (43–24 cm; ca. AD 1650–1860), a large χ_{lf} peak at 43–36 cm coincides with maximum

Table 1 Tephra events from the Rungwe area recorded at Lakes Malawi (Barry et al. 2002) and Masoko (Garcin et al. 2006) during the last 5,000 years

Lake Malawi	Lake Masoko
Tephra A1: age = AD 1674 ± 13 (varve-counting estimate); thickness = 0–1 cm	MKJ-03-II tephra: age = ?; thickness = few mm
Tephra A2: age = AD 1299 ± 78 (varve-counting estimate); thickness = 1 cm	MM-10 tephra: age = AD 790 ± 100 (radiocarbon estimate); thickness = 5–10 cm
Tephra A3: age = 4,350 ± 25 cal. year BP (radiocarbon estimate); thickness = 5–50 cm	Topmost M96-A tephra: age = 4,350 ± 100 cal. year BP (radiocarbon estimate); thickness = 50–100 cm

The correlation between tephras A2 and A3 from lake Malawi with similar tephras, independently dated at Lake Masoko, suggests that the most recent Lake Malawi tephra (i.e. A1) correspond to the Masoko MKJ-03-II tephra

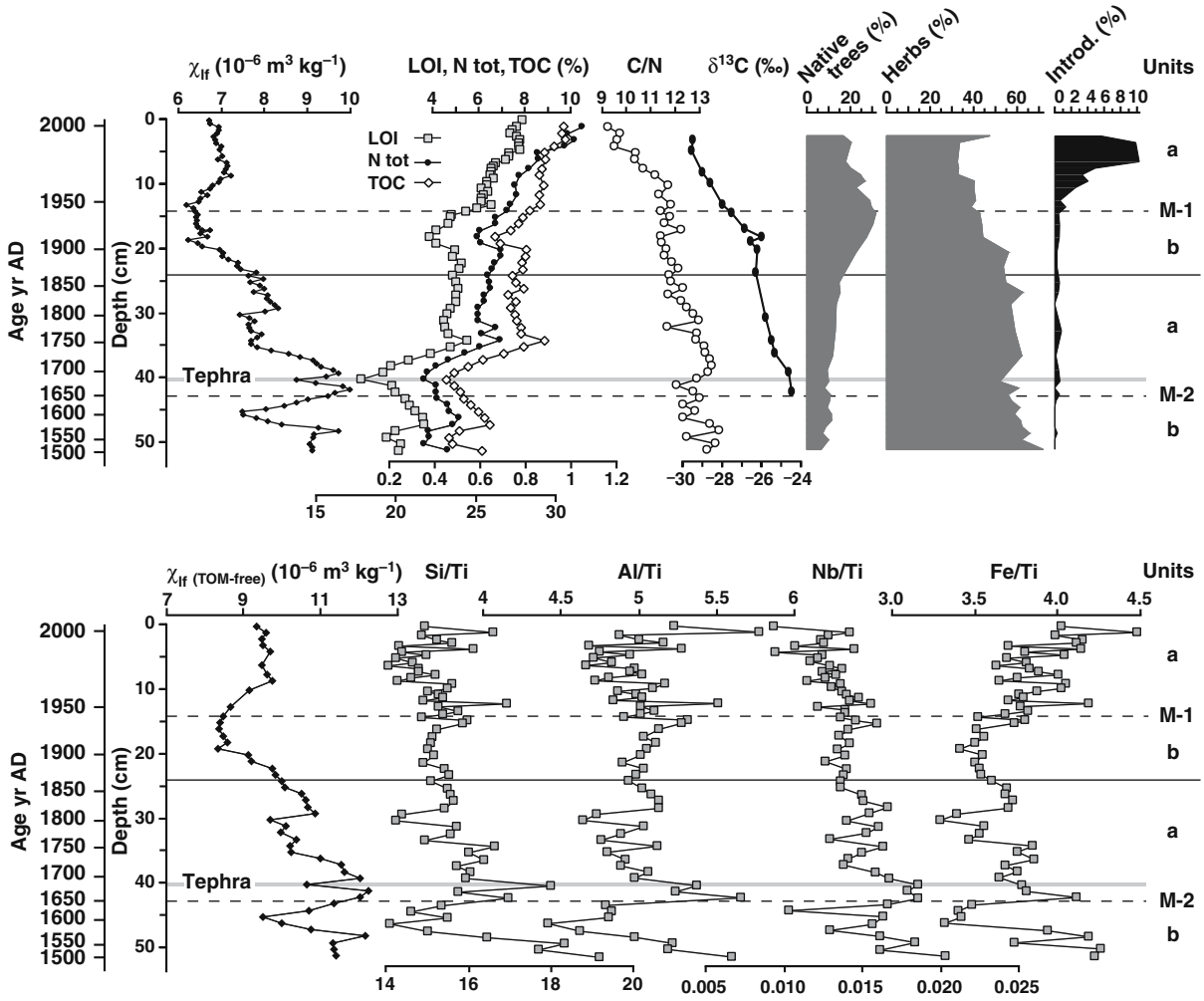

Fig. 4 Multi-proxy profiles from the core MKJ-03-II. Upper panel: profiles χ_{lf}, LOI, N tot, TOC, C/N, $\delta^{13}C$ and pollen content summary (native trees, herbs and introduced taxa). Lower panel: profiles of $\chi_{lf\ (TOM\text{-}free)}$ and geochemical ratio (Si/Ti, Al/Ti, Nb/Ti and Fe/Ti). The resemblance between the χ_{lf} and $\chi_{lf(TOM\text{-}free)}$ profiles shows that the Masoko magnetic signal does not represent the dilution of a clastic source by organic matter. Instead, it represents the input changes of the coarse titanomagnetite from the lakeshore to the deep lake

values in Si/Ti, Al/Ti, Nb/Ti and Fe/Ti ratios, and minimum values of the organic content indicators (LOI, N tot and TOC). From 36 cm upward, χ_{lf} decreases, reaching a minimum at 32 cm. Similar trends are observed in the Si/Ti, Al/Ti, Nb/Ti and Fe/Ti profiles. The tree pollen percentages increase slightly in this sub-unit.

In the upper M-1 unit (24–0 cm; ca. AD 1860–2003) there is a marked increase in native arboreal pollen and relatively low χ_{lf} values. With the exception of the upper 8 cm, the different environmental proxies have lower variability than in unit M-2. In addition, asynchronous changes are observed among the sedimentological and geochemical proxies.

M-1_b (24–14 cm; ca. AD 1860–1940) is characterized by a general decrease of χ_{lf}, which reaches its lowest values (6.4×10^{-6} m^3 kg^{-1}) at the top of this sub-unit. The native tree pollen frequencies increase in this interval, reaching the maximum value (30%) of the record at 15 cm (ca. AD 1930). The geochemical ratios remain stable.

In M-1_a (14–0 cm; ca. AD 1940–2003), the χ_{lf} increases between 14 and 8 cm depth (ca. AD 1970). In contrast with the unit M-2, where high χ_{lf} values correspond to relatively high Si/Ti, Al/Ti, Nb/Ti ratios, these ratios decrease to minimum values at 8 cm depth. The native tree pollen frequencies decrease significantly, when an increase of introduced, cultivated or weed plant pollen (e.g. Cupressaceae, *Euphorbia hirta*, *Arachis hypogaea*, *Eucalyptus*, *Elaeis guineensis*, *Pinus*, *Secale cereale* and *Zea mays*) is observed. These latter taxa reach a maximum (ca. 10%) in the upper 7 cm, i.e. since ca. AD 1980. The highest values of LOI, N tot and TOC and the lowest C/N ratio and $\delta^{13}C$ values are observed in the uppermost sediments, indicating a recent enhancement in poorly degraded, nitrogen-rich organic material.

Changes in sediment sources

The Masoko sediments consist of homogeneous organic silty muds, enriched in amorphous or poorly crystallized glass shards and allophanes, deposited in a suboxic environment where lacustrine biogenic components (mostly silica and organic matter) associated with inorganic and organic terrigenous components are well preserved. To compare the sediment geochemistry with that of the catchment rocks and soils (tuff, soil and eroded soil, see Table 2) and to identify the major changes in sediment content independently of the organic content, the total Si, Al, Nb and Fe contents were normalized to titanium, a lithogenic and relatively immobile element from the surrounding rocks.

The Si/Ti ratio values are significantly higher in the sediments than in the catchment rocks. This is consistent with the preferential weathering of pumice and amorphous silica from the Masoko tuff ring, and its subsequent trapping as colloidal and/or biogenic silica in the lake. The Al/Ti values show the same trends, suggesting a relative enhancement in Al-bearing, poorly crystallized clayey material originating from the catchment weathering (e.g. allophanes), and/or the occurrence of an aeolian and remote Al-rich sediment source.

The Fe/Ti and Nb/Ti ratios of catchment sources and lake sediments show the same range of variation. In the Masoko catchment, the Fe/Ti ratio shows slightly higher values in the unweathered parent tuff, where titanium-poor iron minerals such as magnetite are well preserved (Williamson et al. 1999). Conversely, the Nb/Ti ratio ranges from 0.009 ± 0.004 (9 mg g^{-1}) for the parent tuff material to 0.015 ± 0.003 (15 mg g^{-1}) for the soil, indicating a significant effect of soil weathering and volcanic glass dissolution on the Nb/Ti ratio. This is not surprising, as incompatible elements such as niobium are relatively enriched in the volcanic glass matrix in comparison to titanium or iron. The Nb/Ti ratio values of soils and sediments at Masoko are in the same range as the Nb/Ti ratio values (< 20 mg g^{-1}) recorded in Lake Malawi for the last 700 years (Brown and Johnson 2005). With the exception of volcanic ash fallout, this ratio is initially enriched in soils from the Rungwe area and therefore provides a robust indicator for regional soil input in the nearby lake sediments, including northern Lake Malawi.

The geochemical changes in the sediments may originate from variations in the relative contribution of catchment material (tuff and soil), dependent on pedogenic and transportation pro-

Table 2 χ_{lf} and geochemical properties of the Masoko sediment and catchment material (S.D. = standard deviation)

Material	Samples (n)	χ_{lf} (m^3 kg^{-1})		Si/Ti		Al/Ti		Nb/Ti		Fe/Ti	
		Mean	S.D.	Mean	S.D.	Mean	S.D.	Mean	S.D.	Mean	S.D.
Tuff	12	1.0×10^{-5}	4.6×10^{-6}	9.7	3.4	4.1	0.8	0.009	0.004	3.8	0.5
Soil	19	1.5×10^{-5}	2.2×10^{-6}	10.0	1.5	4.3	0.3	0.015	0.003	3.3	0.2
Eroded soil	2	–	–	14.2	1.2	4.6	0.2	0.009	0.002	4.4	0.3
Lake sediments	66	7.5×10^{-6}	1.0×10^{-6}	15.5	1.0	5.0	0.2	0.015	0.002	3.7	0.3

Erosion soil samples are suspended material from the catchment area collected with a sediment trap

cesses, and perhaps also on aeolian sources. Si/Ti appears two times lower in the catchment materials than in the lake sediments, suggesting that the Si element is strongly depleted by chemical weathering. The other geochemical ratios (Al/Ti, Nb/Ti and Fe/Ti) show almost the same variation in the catchment materials and in the lake sediments, implying that Al, Nb and Fe are more affected by changes of sediment sources, physical erosion and transportation processes (runoff or aeolian inputs) than by chemical weathering. In general, a reduction in physical transportation processes would cause relatively lower values of Si/Ti, Al/Ti, Nb/Ti and Fe/Ti, except during a period of relatively strong chemical weathering. The absence of significant changes in Al/Ti and Fe/Ti values in the lake catchment suggests that these parameters could indicate aeolian inputs into the lake or authigenic deposits associated with changes in the lake chemistry.

Indicators of lake-level dynamics

We used the mass normalized magnetic susceptibility (χ_{lf}, Fig. 4) as a proxy for the concentration of detrital (Ti-)iron oxides held in the terrigenous clastic inputs, primarily controlled by the lake-level dynamics. Hysteresis loop and field-dependence susceptibility measurements, thermomagnetic curves, scanning electron microscope observations and geochemical analyses performed on both catchment materials and lake sediments indicate that the χ_{lf} signal originates from the coarse ca. 20–500 μm multi-domain titanomagnetite ($Fe_{3-x}Ti_xO_4$) (Williamson et al. 1999; Garcin et al. 2006). Due to the high concentration (>1% dry mass) of well preserved detrital titanomagnetite in the lake sediment, secondary magnetic sources associated with the authigenesis of iron oxides, sulfides or carbonates (e.g. see Williamson et al. (1998)) or aerosol fallout form only a small part of the sediment χ_{lf} signal. The titanomagnetite (volumic mass: ca. 5,000 kg m^{-3}) originates from the crater parent rocks and concentrates on the lakeshore (Fig. 5). Observations taken from the lake-catchment suggested that the transfer of titanomagnetite to the deep lake is primarily constrained by changes in lake-level. Indeed, the strong hydraulic conductivity of the catchment materials (>1 m h^{-1}) associated with the small catchment area (20 ha against 36 ha for the lake surface area) makes any impact of runoff erosion processes on the crater-slopes negligible today. In contrast, modern observations show that high amplitude seasonal lake-oscillations coupled with wind-driven turbulence on the lakeshore during the relatively cool and dry winter allow the transport of the titanomagnetite to the deep lake. Lake lowstands act in the same way because they reduce the distance between the lakeshore terrigenous source and the deep lake, thus enhancing the supply of dense and coarse catchment material. These observations are supported by the distribution of modern-sediment χ_{lf}, which indicates a decreasing trend of susceptibility as the distance from the clastic source and the lake depth increase (Fig. 5). Therefore, the sediment χ_{lf} can be interpreted in terms of hydrological regime: high χ_{lf} indicates strong seasonal lake fluctuations and/or lake lowstands, while low χ_{lf} indicates low seasonal lake fluctuations and/or lake highstands.

During the recent period (at least the last 60 years, see below), anthropogenic disturbances on the Masoko basin (i.e. increase of agricultural activity, forest clear cutting and road

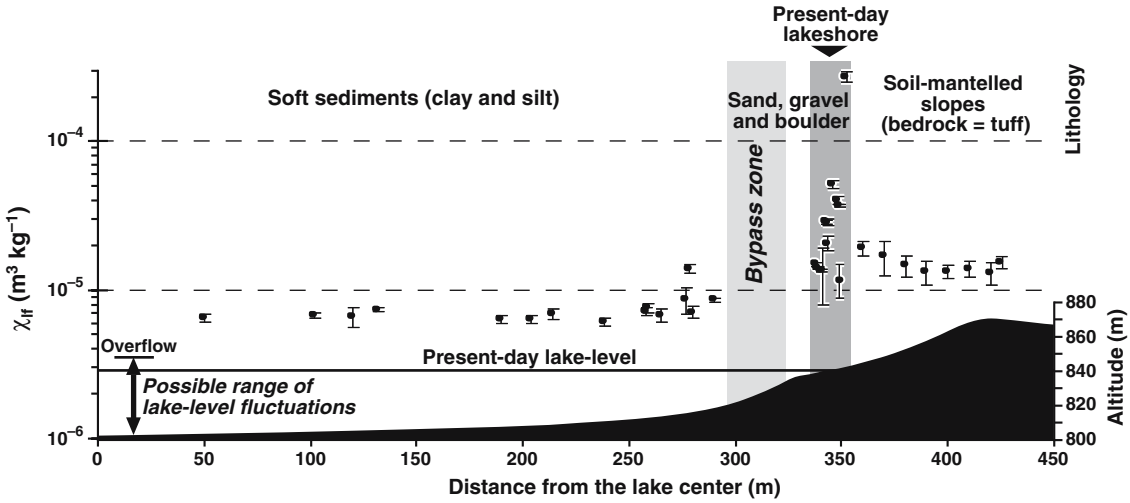

Fig. 5 Relationship between the χ_{lf} (black dots) and the basin morphology. The position of the lakeshore controls the supply of titanomagnetite to the deep lake. Basin lithologies are indicated at the top

construction) creating openings in the natural local vegetation may have modified the inputs of magnetic particles into the lake.

PCA applied to core MKJ-03-II

PCA was used to assess the dominant signal present in the different indicators and to make a synthesis of the relationships between sedimentary parameters and climatic/environmental changes (Fig. 6a). This analysis was performed on the correlation matrix of the three pollen curves (% native trees, % herbs, % introduced taxa), the χ_{lf}, LOI, TOC, and geochemical-petrogenic proxies (Si/Ti, Al/Ti, Nb/Ti and Fe/Ti). The first PC axis (PC1) explains 55% of the total variance,

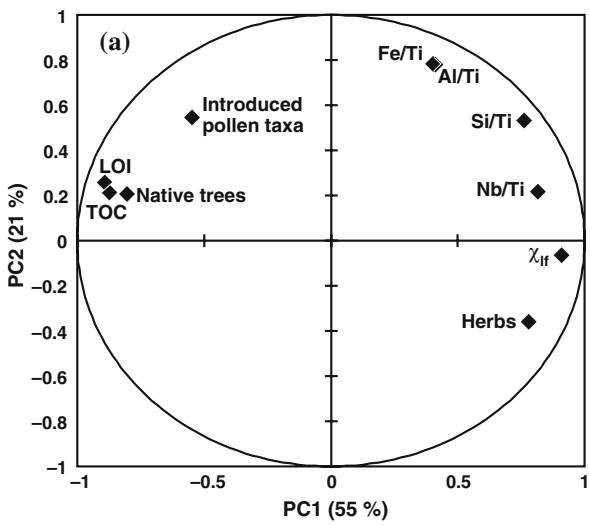

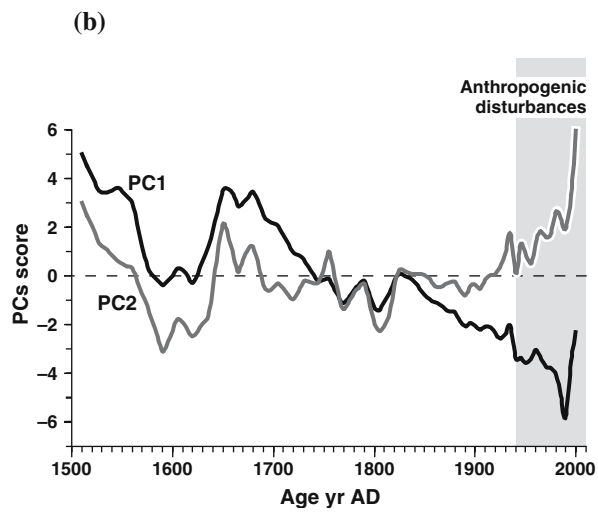

Fig. 6 PCA based on the proxies from core MKJ-03-II. Analysis was made with *XLSTAT*® software. (**a**) Plot of eigenvectors. (**b**) Scores of principal components (PCs). PC1 (black line) and PC2 (grey line) vary in phase from AD 1510 to AD 1940, after which the co-variation breaks down, probably due to anthropogenic disturbances on the crater basin (vertical grey band)

and is positively correlated with the χ_{lf}, Si/Ti and Nb/Ti ratios and the herbs, and negatively correlated with the native trees, introduced taxa and organic proxies (TOC and LOI). This axis reflects changes in lake ecosystem and hydrology: the expansion of herbs in the catchment and the increase in titanomagnetite, Si and Nb inputs to the lake are consistent with dry conditions and increased terrigenous inputs from soils, while the expansion of a tree cover and the deposition of organic matter is consistent with wet conditions. The second PC axis (PC2) explains 21% of the total variance, and is strongly and positively correlated with ratios of Al/Ti, Fe/Ti, Si/Ti and introduced pollen taxa. The correlation with Al/Ti and Fe/Ti ratios suggests that positive values on the second PC axis represent varying inputs from authigenic or atmospheric sources. Both PC1 and PC2 are also associated, although with opposite signs, to frequencies of introduced pollen taxa, which characterize an anthropogenic impact.

Lake Masoko climate and hydrology during the past 500 years

ca. AD 1500–1650 (sub-unit M-2$_b$)

During this period, the Masoko sedimentary basin appears to be tightly coupled to fluctuations in the water-table, which are currently controlled by the strong seasonal contrast of rainfall. High χ_{lf} values and low organic content in this sub-unit indicate high amplitude seasonal lake fluctuations and/or a lake lowstand, consistent with the low frequencies of native tree pollen, which suggest relative open and dry conditions (Fig. 4). A susceptibility minimum centred on AD 1600 (45 cm) may reflect a short wet period. Synchronous changes in Si/Ti, Al/Ti, Nb/Ti and Fe/Ti ratios (Fig. 4) and in the resulting PC1 and PC2 profiles (Fig. 6b) suggest that dissolved and clastic deposition from catchment, lake or remote sources closely follow the change in lake-level dynamics, with maximum inputs during the dry periods, and lower inputs during the relatively wet AD 1600 period.

ca. AD 1650–1860 (sub-unit M-2$_a$)

The relatively high χ_{lf} values and low native tree pollen frequencies (Fig. 4) suggest that this interval corresponds to a generally dry period with low lake-levels and/or high amplitude lake-level fluctuations, with the driest conditions between AD 1650 and AD 1730 as indicated by the maximum values of χ_{lf} and the lowest values of organic content. The relatively high values of Si/Ti, Al/Ti, Fe/Ti, and Nb/Ti at this time suggest an increased deposition of terrigenous material (Fig. 4). Between ca. AD 1730 and 1780 (36–30 cm), however, a decrease in χ_{lf} values synchronous with an increase in organic content could be attributed to a brief wet period. Al/Ti, Fe/Ti and Nb/Ti closely follow this wet period, indicating a rapid decline in the input of soil and possibly aeolian material. The final increase in terrigenous inputs from the catchment (shoreline, soil and tuff material) from ca. AD 1800 suggests that there was a subsequent return to dry conditions and associated transportation processes until ca. AD 1860.

ca. AD 1860–1940 (sub-unit M-1$_b$)

The general decrease in χ_{lf} across this period, in phase with the increase of the native tree pollen frequencies (Fig. 4), indicates both a decrease in fluctuations of the lake-levels and/or a lake highstand, and wetter conditions. The wettest conditions are reached between ca. AD 1900 and 1940, supported by high rainfall amounts observed during the 1920's (Fig. 2). The relative absence of significant changes in sediment geochemistry could reflect a period of stability in the catchment. The local development of a more dense arboreal cover would have prevented significant physical erosion on the basin surface, while the input of dissolved and particulate material from soils would have been buffered by the terrestrial biological cycle. However, the slight increases in Si/Ti and Al/Ti suggest that processes associated with soil weathering and/or potential aeolian inputs, remained active during this period.

ca. AD 1940–2000 (sub-unit M-1$_a$)

The most recent period is characterized by marked human activities on the Masoko basin, where relatively humid conditions persisted until the end of the seventies (Fig. 2). This impact is most clearly seen in the PCA scores: the first two axes co-vary prior to AD 1940, after which they are anti-correlated (Fig. 6b). This change is due to increasing frequencies of introduced taxa, which are negatively correlated with PC1 and positively correlated with PC2. After AD 1940, the increase in PC2 indicates that both hydrologic and pedogenic processes were affected by anthropogenic impact. The development of agricultural activity on the southernmost part of the Masoko basin and on the crater crest (Fig. 1b) is highlighted by the sharp increase in introduced plant taxa and the tree cover decrease, which becomes especially obvious after ca. AD 1980 (Fig. 4). The increased sedimentation of organic matter during this period could also be linked to a variety of anthropogenic perturbations in the catchment. Increasing land use activities such as animal husbandry within the crater, deforestation of the top rim area for cropping, episodic clearing of the woodland on the steepest slopes for charcoal production, deviation of runoff water from the crater surrounding-tracks, and the recent use of fertilizers will have resulted in an increase in nutrient inputs, lake primary production and clastic inputs. The progressive decline of C/N ratio and $\delta^{13}C$ towards the top of the record could therefore be due to a combination of incomplete diagenesis effects and the recent increase in autochthonous organic matter production (mainly aquatic plants and phytoplankton).

The χ_{lf} signal was probably strongly affected by these human disturbances, regardless of any potential iron early diagenesis in the uppermost sediments of this deep and stratified lake. Such an effect probably occurs near the oxycline, ca. 20 m above the lake floor, and should therefore result in an authigenic signature. Current observations show that detrital titanomagnetite grains are the main carriers of the χ_{lf} signal, restricting the effect of authigenesis. There is a general increase in χ_{lf} between ca. 1940 and 1970, followed by a period of stable values that lasts until the present day, suggesting increased shoreline and soil erosion on the basin. This is most probably a result of pastoral activities over the last few decades, development of a track network around the lake, combined with relatively higher interannual climate variability and drier conditions during the last two decades (Fig. 2a).

In the upper sediments, there is a synchronous increase in geochemical proxies of sediment sources (Si/Ti, Al/Ti and Nb/Ti), consistent with strengthened (and unprecedented) soil incision by cattle paths and tracks in the Masoko basin, either as a result of recent crop cultivation and/or relatively drier conditions, which have lowered the average lake-level by about 2–3 m during the last two decades (Luifua village council, personal communication).

Discussion

The Little Ice Age was a prolonged period of cooling lasting from approximately the 16th to the mid-19th centuries. In the Northern Hemisphere this cooling represented less than 1°C (Jones et al. 1998; Mann 2002). In Africa, it appears to have had greater amplitude. Studies of the Ethiopian mountain vegetation indicate a maximum cooling of 2°C (Bonnefille and Mohammed 1994). The oxygen-isotope data from the Mount Kilimanjaro ice cores suggest cold and/or wet conditions (Thompson et al. 2002), and the Mount Kenya moraines indicate a glacier advance (Karlén et al. 1999). Further south, oxygen-isotope data from stalagmites in the Makapansgat Valley, South Africa, suggest a cooling up to 1°C through the LIA (Holmgren et al. 2001).

According to our results, the Masoko area was drier during most of the LIA than during the 20th century. To the south (9.5–14.5°S), sediment cores from the Lake Malawi have revealed similar climatic conditions (Owen et al. 1990; Johnson et al. 2001; Brown and Johnson 2005) (Fig. 7e). An erosional hiatus that occurred between about AD 1500 and 1800, was interpreted as a ca. 120 m lake-level drop (Owen et al. 1990). This lake lowstand period is correlated with the dry period of Lakes Chilwa and Chiuta (located 100 km southeast of Lake Malawi) (Owen and Crossley

1990). Lowstands have been also observed during the LIA at Lake Tanganyika (3–9°S), located slightly to the north of Masoko, from AD 1500 until AD 1580, and from ca. AD 1650 until the end of the 17th century, where the lowest lake-levels are inferred (Cohen et al. 1997; Alin and Cohen 2003). Relatively low levels persist until AD 1830, and are followed by a transgression that culminated at the end of the 19th century (Fig. 7d). In contrast, further north, evidence from Lakes Naivasha (0.7°S) and Victoria (2.5°S–0.5°N) indicates relatively wet conditions with high lake-levels during the LIA, interrupted by short drought periods (Verschuren et al. 2000; Verschuren 2004; Stager et al. 2005) (Fig. 7a, b). This apparently contrasted North-South climatic pattern, however, is not observed at Lake Edward, where dry conditions during the 16th and 17th centuries have been inferred (Russell and Johnson 2005) (Fig. 7c).

These regional discordances highlight possible contrasted climatic conditions between East and austral Africa in the recent past (Tyson et al. 2002). Among the potential causes, the El Niño-Southern Oscillation (ENSO) phenomenon could have been the main trigger mechanism of these regional discordances. According to Goddard and Graham (1999), at the interannual scale, ENSO affects the Indian Ocean sea surface temperatures and in turn the moisture flux over central-eastern and austral Africa. During El Niño-like events, the western Indian Ocean warms, producing an anomalously convergent moisture flux (wetter conditions) over central East Africa and drier conditions over austral Africa. During La Niña-like events these changes are approximately reversed. The Lake Masoko belongs to the region affected by ENSO-teleconnected droughts, with generally dry conditions during El Niño events and wet conditions during La Niña events (Fig. 2b).

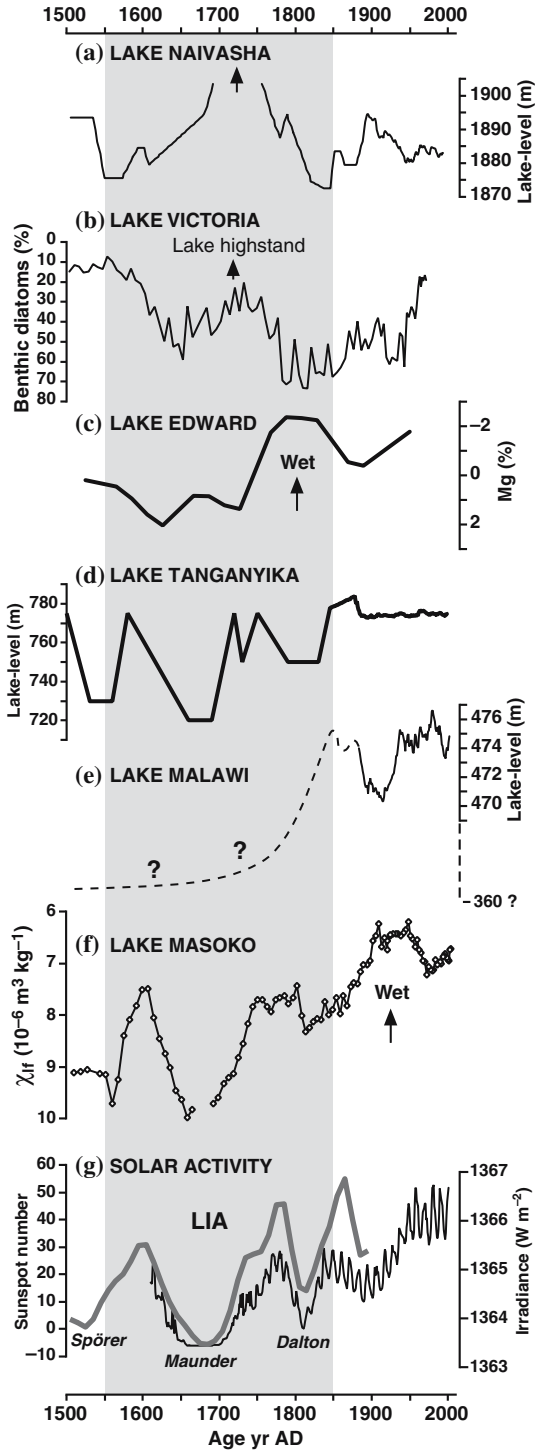

Fig. 7 Comparison of the Masoko crater history with reconstructed climate-proxy data for the last 500 years. (**a**) Lake Naivasha levels (Verschuren et al. 2000), (**b**) Lake Victoria levels (Stager et al. 2005), (**c**) Lake Edward Mg (%): proxy of lake-level (Russell and Johnson 2005), (**d**) Lake Tanganyika levels (Cohen et al. 1997; Alin and Cohen 2003), (**e**) Lake Malawi levels (Owen et al. 1990), (**f**) Lake Masoko χ_{lf}, and (**g**) solar activity: the thin line shows the irradiance reconstruction since AD 1600 (Lean 2000) and the thick line shows the long-term variation of sunspot numbers (Solanki et al. 2004). LIA is the 'Little Ice Age' climatic period, highlighted by a grey band

During the last millennium, both Lake Naivasha and Lake Victoria show a negative correlation between solar activity and lake-levels that ends during the Dalton minimum (ca. AD 1800), while subsequently and today, this correlation is positive (Verschuren et al. 2000; Stager et al. 2005). Pioneering studies dealing with the relationship between solar activity and African lake-levels were initiated during the 1920's. Brooks (1923) found that the levels of Lakes Victoria and Albert were correlated with sunspot number for the years AD 1896–1922. Dixey (1924) also found this relationship on the Lake Malawi, for the same period of measurements. However, at Lake Malawi, this relationship was weaker over the following period (AD 1922–1940) and was questioned by Kanthack (1941). Instrumental records from the end of the 19th century at Lakes Naivasha and Malawi indicate a strong negative correlation of these two lakes (Verschuren 2004). This observation suggests that for the last 120 years at least, Lakes Naivasha and Malawi have belonged to two different climatic patterns.

Lake Masoko is located in the Rungwe Mountains, at the northern end of Lake Malawi catchment. This area is known to be one of the main sources of water for Lake Malawi (Kerr-Cross 1891; Branchu et al. 2005), conveyed through the Songwe, Kiwira, Mbaka and Lufira perennial rivers. From this relation, it may be expected that the levels of Lakes Masoko and Malawi should vary in-phase. The inferred hydrological changes at Masoko indicate a general dry period during the LIA, as observed at Lake Malawi. Further, these changes are in phase with the solar activity cycles (Fig. 7f, g). During the Sporër, Maunder and Dalton minima of solar activity, climatic conditions were probably drier than today in the Lake Masoko area.

At the scale of the whole tropical region, dry conditions are observed in the northern part of South America during the LIA, where they are attributed to a southward shift of the ITCZ mean position (Haug et al. 2001), in phase with the decrease in monsoon precipitation recorded in southern Oman (Fleitmann et al. 2004). However, during the same period in East Africa, Lakes Naivasha and Victoria show wet conditions (until ca. AD 1800) in the equatorial region, while Lakes Tanganyika, Masoko and Malawi to the south show dry conditions. The pattern of wetter conditions near the equator (with the exception of Lake Edward) and drier conditions in the southern tropics, if associated with the migration of mean position of the ITCZ, may indicate an equatorward contraction (reduction of the seasonal migrations) of the ITCZ in East Africa during this period of minimum solar activity. Such a scenario is partly supported by the results of climate modelling experiments that simulate the tropical atmosphere system under differential outputs of the Sun (Balachandran et al. 1999).

More recently, anthropogenic impacts are clearly identified on the Masoko basin since the 1940's. This observation confirms the major human disturbances previously reported in East African lakes from the second half of the 1900's. For example, the unprecedented rates of sedimentation during the early 1960's in the Lake Tanganyika basin suggest strong disturbances, which involve a combination of climatic and anthropogenic causes (e.g. heavy rainfall and deforestation) (Cohen et al. 2005). In Lake Haubi (central Tanzania), soil erosion increased from 1935 onward, with high rates between ca. 1945 to the present (Eriksson and Sandgren 1999). Similarly, human population growth and agricultural activity around Lake Victoria has led to an eutrophication of the lake from the 1960's (Verschuren et al. 2002). As Calder et al. (1995) observed in the Lake Malawi catchment between 1967 and 1990, the recent deforestation in the Lake Masoko area has probably lowered forest interception and increased runoff. Further work is needed to improve the understanding of specific human controls (e.g. animal husbandry, clear cutting, shore occupation, agriculture) on sediment deposition in Lake Masoko over the last 60 years.

Conclusion

Lake Masoko provides new insights into environmental and climatic changes for the last

500 years in southern East Africa. The multi-proxy study performed on the core MKJ-03-II shows several marked changes in the sedimentary content, which are interpreted in term of lake-level, climatic changes and anthropogenic disturbances.

Prior to the 1940's, catchment erosion, weathering and lake deposition processes at Masoko were strongly associated with lake-level fluctuations, with maximum soil transportation during relatively dry periods. During the Little Ice Age, the Masoko area was drier than today, in agreement with the regional data obtained from Lakes Malawi and Tanganyika. In contrast, the equatorial Lakes Naivasha and Victoria to the northeast show opposite hydrological changes (until ca. AD 1800). These regional climatic contrasts between south and equatorial latitudes are confirmed by the instrumental measurement of lake-levels since the end of the 19th century. Inferred changes of the Masoko hydrology are positively correlated with the solar activity proxies. This implies a forcing of solar activity on the atmospheric circulation and thus on the regional climate of this part of East Africa, confirming the suggestions previously made for equatorial East Africa through the studies of Lakes Naivasha and Victoria. From ca. AD 1940 onward, the development of land use activities near the lake has strongly modified the depositional environment of the Masoko crater. Whilst catchment erosion and weathering processes still played an important role on the deposition, the long term climatic forcing on such local processes was biased by the impact of human activities, which has become increasingly strong over the last 60 years.

Finally, alternative dating techniques are needed to verify or corroborate the chronological framework of non-annually varved sediments, mainly based on ^{14}C and ^{210}Pb dating techniques. This study raises the interest of tephra layers originating from the volcanic areas of the African rift, which provide instantaneous temporal marker layers over a wide spatial area (i.e. volcanic ash layers). The detection of these recent volcanic events in the sedimentary record could be used to develop a tephrochronology database, and to improve the chronology of regional climate records for the last millennium.

Acknowledgements A. Issah, E. Mwandapile, S. Kajula, B. Gwambene and M. Decobert are thanked for assisting us during fieldwork at Lake Masoko in 2003, 2004 and 2005. We acknowledge P. Valimba for providing Musekera rainfall data. We also thank A.S. Cohen and J.M. Russell for many valuable comments on an earlier version of this manuscript. This research was supported by the Tanzania Commission for Science and Technology (COSTECH), the CLEHA project of the ECLIPSE program (Institut National des Sciences de l'Univers), the RESOLVE project of the ACI Ecologie Quantitative program (Ministère Français de la Recherche), and the ARTEMIS project.

References

Alin SR, Cohen AS (2003) Lake-level history of Lake Tanganyika, East Africa, for the past 2500 years based on ostracode-inferred water-depth reconstruction. Palaeogeogr Palaeoclimatol Palaeoecol 199:31–49

Balachandran NK, Rind D, Lonergan P, Shindell DT (1999) Effects of solar cycle variability on the lower stratosphere and the troposphere. J Geophys Res 104:27321–27340

Barker P, Telford R, Merdaci O, Williamson D, Taieb M, Vincens A, Gibert E (2000) The sensitivity of a Tanzanian crater lake to catastrophic tephra input and four millennia of climate change. Holocene 10:303–310

Barker P, Williamson D, Gasse F, Gibert E (2003) Climatic and volcanic forcing revealed in a 50,000-year diatom record from Lake Massoko, Tanzania. Quat Res 60:368–376

Barry S, Filippi ML, Talbot MR, Johnson T (2002) Sedimentology and geochronology of Late Pleistocene and Holocene sediments from Lake Malawi. In: Odada EO, Olago DO (eds) The east African great lakes: limnology, palaeolimnology and biodiversity. Kluwer Academic Publishers, Dordrecht, Netherlands, pp 369–391

Bergonzini L, Gibert E, Winckel A, Merdaci O (2001) Water and isotopic (^{18}O and ^{2}H) budget of Lake Massoko, Tanzania. Quantification of exchange between Lake and groundwater. C R Acad Sci Paris 333:617–623

Binford MW, Kahl JS, Norton SA (1993) Interpretation of ^{210}Pb profiles and verification of the CRS dating model in PIRLA project lake sediment cores. J Paleolimnol 9:275–296

Bonnefille R, Mohammed U (1994) Pollen-Inferred Climatic Fluctuations in Ethiopia During the Last 3000 Years. Palaeogeogr Palaeoclimatol Palaeoecol 109:331–343

Branchu P, Bergonzini L, Delvaux D, De Batist M, Golubev V, Benedetti M, Klerkx J (2005) Tectonic, climatic and hydrothermal control on sedimentation and water chemistry of northern Lake Malawi (Nyasa), Tanzania. J Afr Earth Sci 43:433–446

Brooks CEP (1923) Variations in the levels of the Central African Lakes Victoria and Albert. Geophys Mem 20:1–9

Brown ET, Johnson TC (2005) Coherence between tropical East African and South American records of the Little Ice Age. Geochem Geophys Geosyst 6: Q12005, doi:10.1029/2005GC000959

Calder IR, Hall RL, Bastable HG, Gunston HM, Shela O, Chirwa A, Kafundu R (1995) The impact of land-use change on water-resources in sub-Saharan Africa—a modeling study of Lake Malawi. J Hydrol 170:123–135

Cohen AS, Palacios-Fest MR, Msaky ES, Alin SR, McKee B, O'Reilly CM, Dettman DL, Nkotagu H, Lezzar KE (2005) Paleolimnological investigations of anthropogenic environmental change in Lake Tanganyika: IX. Summary of paleorecords of environmental change and catchment deforestation at Lake Tanganyika and impacts on the Lake Tanganyika ecosystem. J Paleolimnol 34:125–145

Cohen AS, Talbot MR, Awramik SM, Dettman DL, Abell P (1997) Lake level and paleoenvironmental history of Lake Tanganyika, Africa, as inferred from late Holocene and modern stromatolites. Geol Soc Am Bull 109:444–460

Delalande M, Bergonzini L, Beal F, Garcin Y, Majule A, Williamson D (2005) Contribution to the detection of Lake Masoko (Tanzania) groundwater outflow: isotopic evidence (^{18}O, D). IAHS Publ 50:867–880

Dixey F (1924) Lake level in relation to rainfall and sunspots. Nature 114:659–661

Eriksson MG, Sandgren P (1999) Mineral magnetic analyses of sediment cores recording recent soil erosion history in central Tanzania. Palaeogeogr Palaeoclimatol Palaeoecol 152:365–383

Fleitmann D, Burns SJ, Neff U, Mudelsee M, Mangini A, Matter A (2004) Palaeoclimatic interpretation of high-resolution oxygen isotope profiles derived from annually laminated speleothems from Southern Oman. Quat Sci Rev 23:935–945

Garcin Y, Williamson D, Taieb M, Vincens A, Mathé PE, Majule A (2006) Centennial to millennial changes in maar-lake deposition during the last 45,000 years in tropical Southern Africa (Lake Masoko, Tanzania). Palaeogeogr Palaeoclimatol Palaeoecol: in press

Gibert E, Bergonzini L, Massault M, Williamson D (2002) AMS-C-14 chronology of 40.0 cal ka BP continuous deposits from a crater lake (Lake Massoko, Tanzania)—modern water balance and environmental implications. Palaeogeogr Palaeoclimatol Palaeoecol 187:307–322

Gillman C (1927) South-west Tanganyika territory. Geogr J 69:97–126

Gillman C (1936) A population map of Tanganyika territory. Geogr Review 26:353–375

Goddard L, Graham NE (1999) Importance of the Indian Ocean for simulating rainfall anomalies over eastern and southern Africa. J Geophys Res Atmos 104:19099–19116

Haug GH, Hughen KA, Sigman DM, Peterson LC, Rohl U (2001) Southward migration of the intertropical convergence zone through the Holocene. Science 293:1304–1308

Holmgren K, Moberg A, Svanered O, Tyson PD (2001) A preliminary 3000-year regional temperature reconstruction for South Africa. S Afr J Sci 97:49–51

Huffman TN (1996) Archaeological evidence for climatic change during the last 2000 years in southern Africa. Quat Int 33:55–60

Johnson TC, Barry SL, Chan Y, Wilkinson P (2001) Decadal record of climate variability spanning the past 700 year in the Southern Tropics of East Africa. Geology 29:83–86

Johnson TC, Brown ET, McManus J (2004) Diatom productivity in Northern Lake Malawi during the past 25,000 years: implications for the position of the Intertropical Convergence Zone at millennial and shorter time scales. In: Battarbee RW, Gasse F, Stickley CE (eds) Past climate variability through Europe and Africa. Springer, Dordrecht, The Netherlands, pp 93–116

Jones PD, Briffa KR, Barnett TP, Tett SFB (1998) High-resolution palaeoclimatic records for the last millennium: interpretation, integration and comparison with General Circulation Model control-run temperatures. Holocene 8:455–471

Kajak Z (1971) Benthos of standing water. In: Edmondson WT, Winberg GG (eds) A manual on methods for the assessment of secondary productivity in fresh waters. Blackwell Scientific Publications, Oxford, pp 25–65

Kanthack FE (1941) The fluctuations of Lake Nyasa. Geogr J 98:20–33

Karlén W, Fastook JL, Holmgren K, Malmstrom M, Matthews JA, Odada E, Risberg J, Rosqvist G, Sandgren P, Shemesh A, Westerberg LO (1999) Glacier fluctuations on Mount Kenya since ~6000 cal. years BP: implications for Holocene climatic change in Africa. Ambio 28:409–418

Kerr-Cross D (1891) Notes on the country lying between Lakes Nyassa and Tanganyika. Proc R Geogr Soc Month Rec Geogr 13:86–99

Krishnaswamy S, Lal D, Martin JM, Meybeck M (1971) Geochronology of lake sediments. Earth Planet Sci Lett 11:407–414

Lean J (2000) Evolution of the sun's spectral irradiance since the Maunder Minimum. Geophys Res Lett 27:2425–2428

Letcher O (1918) Notes on the South-western area of ''German'' East Africa. Geogr J 51:164–172

Mann ME (2002) The value of multiple proxies. Science 297:1481–1482

Merdaci O (1998) Changements climatiques au cours des derniers 30000 ans en Afrique Sud-Equatoriale (Tanzanie) par l'étude des pigments et phénols lacustres. Unpublished PhD Thesis, University Aix-Marseille III, 208 pp

Meyers PA (1994) Preservation of elemental and isotopic source identification of sedimentary organic-matter. Chem Geol 114:289–302

Nicholson SE (1996) A review of climate dynamics and climate variability in eastern Africa. In: Johnson TC, Odada EO (eds) The limnology, climatology and paleoclimatology of the East African lakes. Gordon and Breach Publishers, Amsterdam, pp 25–56

Owen RB, Crossley R (1990) Recent sedimentation in Lakes Chilwa and Chiuta, Malawi. Palaeoecol Afr 20:109–117

Owen RB, Crossley R, Johnson TC, Tweddle D, Kornfield I, Davison S, Eccles DH, Engstrom DE (1990) Major low levels of Lake Malawi and their implications for speciation rates in Cichlid fishes. Proc R Soc London Ser B 240:519–553

Russell JM, Johnson TC (2005) A high-resolution geochemical record from Lake Edward, Uganda Congo and the timing and causes of tropical African drought during the late Holocene. Quat Sci Rev 24:1375–1389

Schnee H (1920) Deutsches Koloniallexikon, Bd. 1. von Quelle and Meyer, Leipzig, 471 pp

Smith TM, Reynolds RW (2004) Improved extended reconstruction of SST (1854-1997). J Clim 17:2466–2477

Solanki SK, Usoskin IG, Kromer B, Schussler M, Beer J (2004) Unusual activity of the Sun during recent decades compared to the previous 11,000 years. Nature 431:1084–1087

Stager JC, Ryves D, Cumming BF, Meeker LD, Beer J (2005) Solar variability and the levels of Lake Victoria, East Africa, during the last millenium. J Paleolimnol 33:243–251

Thevenon F, Williamson D, Vincens A, Taieb M, Merdaci O, Decobert M, Buchet G (2003) A late-Holocene charcoal record from Lake Masoko, SW Tanzania: climatic and anthropologic implications. Holocene 13:785–792

Thompson LG, Mosley-Thompson E, Davis ME, Henderson KA, Brecher HH, Zagorodnov VS, Mashiotta TA, Lin PN, Mikhalenko VN, Hardy DR, Beer J (2002) Kilimanjaro ice core records: evidence of holocene climate change in tropical Africa. Science 298:589–593

Tyson PD, Lee-Thorp J, Holmgren K, Thackeray JF (2002) Changing gradients of climate change in Southern Africa during the past millennium: implications for population movements. Clim Change 52:129–135

Verschuren D (2004) Decadal and century-scale climate variability in tropical Africa during the past 2000 years. In: Battarbee RW, Gasse F, Stickley CE (eds) Past climate variability through Europe and Africa. Springer, Dordrecht The Netherlands, pp 139–158

Verschuren D, Johnson TC, Kling HJ, Edgington DN, Leavitt PR, Brown ET, Talbot MR, Hecky RE (2002) History and timing of human impact on Lake Victoria, East Africa. Proc R Soc London Ser B 269:289–294

Verschuren D, Laird KR, Cumming BF (2000) Rainfall and drought in equatorial east Africa during the past 1100 years. Nature 403:410–414

Vincens A, Williamson D, Thevenon F, Taieb M, Buchet G, Decobert M, Thouveny N (2003) Pollen-based vegetation changes in southern Tanzania during the last 4200 years: climate change and/or human impact. Palaeogeogr Palaeoclimatol Palaeoecol 198:321–334

White F (1983) The Vegetation of Africa. A descriptive Memoir to Accompagny the UNESCO/AETFAT/UNSO Vegetation Map of Africa, Paris, 356 pp

Williamson D, Jackson MJ, Banerjee SK, Marvin J, Merdaci O, Thouveny N, Decobert M, Gibert-Massault E, Massault M, Mazaudier D, Taieb M (1999) Magnetic signatures of hydrological change in a tropical maar-lake (Lake Massoko, Tanzania): Preliminary results. Phys Chem Earth Pt A Solid Earth Geod 24:799–803

Williamson D, Jelinowska A, Kissel C, Tucholka P, Gibert E, Gasse F, Massault M, Taieb M, Van Campo E, Wieckowski K (1998) Mineral-magnetic proxies of erosion/oxidation cycles in tropical maar-lake sediments (Lake Tritrivakely, Madagascar): paleoenvironmental implications. Earth Planet Sci Lett 155:205–219